UDC 546.73'261'02:541.49

SYNTHESIS, CHARACTERIZATION AND IN SILICO STUDIES OF NEOCUPROINE COMPLEXES WITH COBALT(II)-FORMATE

Safayev Shonazar Oktam o'g'li
Doctoral student of Khorezm mamun academy, Khiva, Uzbekistan
E-mail: shonazar@urdu.uz
Kadirova Shaxnoza Abduxalilovna
Doctor of chemical sciences, head of the chemistry department, National university of Uzbekistan, Tashkent, Uzbekistan
E-mail: kadirva.sh@mail.ru
Abdullayeva Zubayda Shavkatovna
Doctor of philosophy in chemistry, lecturer, Urgench "Ranch" university, Urgench, Uzbekistan
e-mail: zubayda.abdullayeva.91@mail.ru
ODCID: 0000-0001-7810-9012

Abstract. This investigation details the synthesis, characterization, and computational assessment of two innovative cobalt(II)-formate complexes, utilizing neocuproine (neo) as the principal ligand: $Co[(neo)_2(aqua)_2](formate)_2$ and $Co[(neo)_2(urea)_2](formate)_2$. The complexes underwent synthesis and were subsequently characterized through using the technique of infrared (IR) spectroscopy and wavelength-dispersive X-ray fluorescence (WD-XRF) elemental analysis. IR spectroscopy validated the bidentate coordination of neocuproine through its nitrogen atoms, as well as the unique coordination modes of the auxiliary ligands—water molecules in the initial complex and urea through its carbonyl oxygen in the subsequent one. The results of the elemental analysis were in remarkable concordance with the proposed empirical formulas, thereby affirming both high purity and precise quantitative stoichiometry.

Keywords: Cobalt(II) complexes; Neocuproine; Formate; IR spectroscopy; Elemental analysis; Quantum chemical calculations; Molecular docking; CCR1 receptor.

Аннотация. Данное исследование описывает синтез, характеристику и вычислительную оценку двух новых форматных комплексов кобальта(II) с неокупроином (neo) в качестве основного лиганда: $Co[(neo)_2(aqua)_2](formate)_2$ и $Co[(neo)_2(urea)_2](formate)_2$. Комплексы были синтезированы и охарактеризованы методом инфракрасной (ИК) спектроскопии и элементного анализа с помощью волнодисперсионной рентгенофлуоресценции (WD-XRF). ИК-спектроскопия подтвердила бидентантную координацию неокупроина через атомы азота, а также уникальные режимы координации вспомогательных лигандов – молекул

ISSN 3030-3907

воды в первом комплексе и мочевины через карбонильный кислород во втором. Результаты элементного анализа показали замечательное соответствие предложенным эмпирическим формулам, подтвердив как высокую чистоту, так и точную количественную стехиометрию.

Ключевые слова: Комплексы кобальта(II); Неокупроин; Формиат; ИК-спектроскопия; Элементный анализ; Квантово-химические расчеты; Молекулярный докинг; Рецептор CCR1.

Annotatsiya. Ushbu tadqiqot ikki yangi kobalt(II)-format kompleksining sintezi, xarakterlash va hisoblash bahosini tavsiflaydi. Bunda asosiy ligand sifatida neokuproin (neo) ishlatilgan. Komplekslar sintez qilindi va keyin ular infraqizil (IK) spektroskopiya va to'lqinli-dispersiv rentgen-fluoresens (WD-XRF) element tahlili orqali xarakterlandi. IK spektroskopiya neokuproinning azot atomlari orqali ikki bidentat koordinatsiyasini, shuningdek, yordamchi ligandlarning - birinchi kompleksdagi suv molekulalari va ikkinchi kompleksdagi karbamidning karbonil kislorodi orqali - o'ziga xos bog'lanish usullarini tasdiqladi. Element tahlili natijalari taklif qilingan empirik formulalar bilan ajoyib mos keldi, bu aniq miqdoriy stexiometriyani tasdiqladi.

Kalit so‘zlar: Kobalt(II) komplekslari; Neokuporin; Formiat; IR spektroskopiya; Element tahlili; Kvant kimyoviy hisoblashlar; Molekulyar doklash; CCR1 retseptori.

Introduction.

1,10-Phenanthroline (phen) is a well-known bidentate ligand that is often used in coordination chemistry because it can make stable complexes with a wide range of transition metals. The ligand has two nitrogen atoms that can form coordinate bonds. This lets it take on different coordination modes depending on the metal ion and the shape of the resulting complex. Many research studies have documented the synthesis and characterization of coordination compounds containing 1,10-phenanthroline, demonstrating a diverse array of structures and properties.

LITERATURE REVIEW

The use of 1,10-phenanthroline to make coordination compounds can be seen in how it interacts with metal ions like cadmium, copper, manganese, and yttrium. For example, cadmium (II) has been shown to make coordination polymers with 1,10-phenanthroline, which led to the discovery of a new coordination polymer with benzene-1,4-dicarboxylate ligands [1]. These coordination compounds frequently display intriguing structural characteristics and can range in dimensionality from one-dimensional chains to more intricate two- or three-dimensional frameworks, contingent upon the selection of metal ions and supplementary bridging ligands [2-3].

ISSN 3030-3907

Additionally, 1,10-phenanthroline complexes have garnered interest due to their luminescent characteristics. Research has demonstrated that alterations to the phenanthroline structure can result in improved photoluminescence, a characteristic that is especially utilized in the development of luminescent materials [4]. Europium (III) complexes with phenanthroline derivatives have shown good energy transfer and luminescence properties that are very useful in optoelectronic applications [5].

It is important to note that modifying the phenanthroline ligand at certain points in its structure can give it new properties, such as better solubility or specific binding affinities for certain uses, like drug delivery or catalysis. For instance, adding more functional groups can make the ligand bind more strongly to certain metal ions. This is important for making stable metal-ligand systems that can be used in a variety of ways, such as in catalysis [6].

MATERIALS AND METHODS

All chemicals were obtained from commercial suppliers and used without further purification.

Synthesis of. $Co[(neo)_2(aqua)_2](formate)_2$. Neocuproine (5 mmol) was dissolved in ethanol. In a separate vessel, 2.5 mmol of cobalt(II) formate dihydrate was dissolved in deionized water. The neocuproine solution was added dropwise to the aqueous cobalt formate solution while continuously stirring. The resultant mixture was kept at 50 °C with ultrasonic irradiation for 30 minutes. The solution was then filtered and allowed to slowly evaporate at ambient temperature. After 15 days, brownish crystals were formed. Yield: 89%.

Synthesis of. $Co[(neo)_2(urea)_2](formate)_2$. Neocuproine (5 mmol) was dissolved in ethanol. Cobalt(II) formate dihydrate (2.5 mmol) and urea (5 mmol) were mixed together in deionized water. The ethanolic neocuproine solution and a separate aqueous urea solution were both added to the stirred aqueous solution of cobalt formate. The reaction mixture was then submitted to the same process as previously described, with ultrasonication at 50 °C, followed by filtration and slow evaporation. After 15 days, light brownish crystals had been separated. Yield: 92%.

Instrumental studies. Infrared spectroscopy was performed with a Shimadzu IRAffinity-1S fourier transform infrared spectrophotometer. Solid powder samples were evaluated without mixing in KBr and placed in the diffuse reflectance probe's sample cup for measurement. The measurements were taken at room temperature with a wavenumber range of 4000 to 400 cm^{-1}.

The synthesized cobalt complexes were analyzed using a Rigaku ZSX Primus III NEXT sequential wavelength-dispersive X-ray fluorescence (WD-XRF) spectrometer with a 3 kW Rhodium (Rh) target end-window X-ray tube. The spectrometer was operated in a vacuum atmosphere (<30 Pa) to improve light

ISSN 3030-3907

detection. The X-ray tube was set at 50 kV and 50 mA. Each element was analyzed using a combination of sequential scanning and fixed-time counting on specific analytical lines.

Quantum Chemical Studies. All quantum chemistry computations were carried out using the Gaussian 09 software tool. Geometry optimizations, single-point energy calculations, and frequency calculations were performed on the ligands (neocuproine and urea) and cobalt(II) metal complexes. The ligands were calculated using the RB3LYP functional (Becke's three-parameter exchange functional paired with the Lee-Yang-Parr correlation functional) and the 3-21G basis set. The ligands were modeled as neutral species with a singlet spin state, which matched their closed-shell structures.

For the cobalt(II) metal complexes, the same RB3LYP/3-21G level of theory was used. These open-shell systems were defined as having a total charge of +2, corresponding to the Co(II) ion, and a doublet spin multiplicity. All computations were performed in the gas phase, with no solvation model. All optimized geometries were subjected to frequency calculations at the same level of theory to ensure they represented real minima on the potential energy surface and to derive thermodynamic attributes.

Molecular Docking Procedures. Ligand and Receptor Preparation The 3D structures of the docking ligands, $Co[(neo)_2(aqua)_2](formate)_2$ and $Co[(neo)_2(urea)_2](formate)_2$, were quantum mechanically optimized using Gaussian 09. Kollman charges were subsequently added to the ligands using AutoDock Tools.

The crystal structure of the CCR1 receptor was acquired from the Protein Data Bank (PDB). The receptor underwent preparation through the elimination of side chains, the initial co-crystallized ligand, and solvent molecules. Subsequently, polar hydrogens and charges were incorporated into the protein structure.

Protocols for Docking Two distinct docking studies were conducted. At the outset, a study focused on cavity detection to facilitate blind docking was performed utilizing the CB-Dock2 web-based service. Subsequently, an independent docking analysis was conducted utilizing AutoDock Vina. The outcomes derived from the two docking methodologies were compared in order to validate the conclusions that were drawn.

RESULTS AND DISCUSSION

The results and discussion of the infrared spectroscopy analysis. The interpretation of the infrared spectra for the metal complexes first necessitated a thorough analysis of the characteristic vibrational modes of the free ligands, urea and neocuproine, to establish a baseline for identifying coordination-induced shifts.

ISSN 3030-3907

The IR spectrum of free urea (Figure 1) displays the expected signature peaks for this molecule. The most diagnostically significant vibration is the strong carbonyl (C=O) stretching mode, observed at 1660.26 cm^{-1}. This peak is highly sensitive to the electronic environment of the oxygen atom and is thus a critical probe for metal coordination. Furthermore, the spectrum shows a series of sharp peaks in the high-frequency region at 3503.10 cm^{-1}, 3372.29 cm^{-1}, and 3265.73 cm^{-1}, which are assigned to the asymmetric and symmetric N-H stretching vibrations. Coordination of urea to a metal center, typically through its carbonyl oxygen, is expected to weaken the C=O bond due to the donation of electron density from the oxygen lone pair to the metal, resulting in a measurable shift of this stretching frequency to a lower wavenumber [7- 8]. Concomitant shifts in the N-H stretching region are also anticipated due to changes in hydrogen bonding and the electron-withdrawing effect of the coordinated metal.

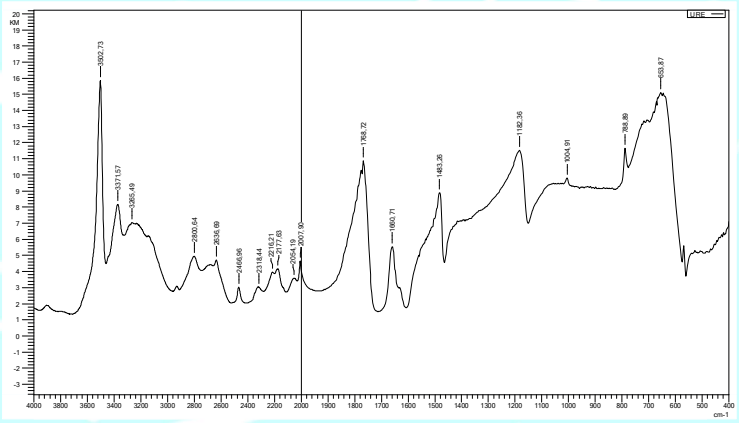


Figure 1. Infrared spectra of urea

The IR spectrum of free neocuproine (2,9-dimethyl-1,10-phenanthroline) (Figure 2) reflects its aromatic nature. The key vibrations for assessing coordination are found in the fingerprint region between 1400 and 1650 cm^{-1}, which arises from the C=C and C=N stretching modes of the phenanthroline ring system. Prominent peaks in this region are observed at 1613.97 cm^{-1}, 1591.57 cm^{-1}, 1550.16 cm^{-1}, 1504.38 cm^{-1}, and 1495.24 cm^{-1}. As a classic bidentate chelating ligand, neocuproine coordinates to metal ions through its two nitrogen atoms. This coordination alters the electron density within the heterocyclic ring, leading to shifts in the energies of these ring-stretching vibrations [9]. The confirmation of coordination is often based on observable changes in the pattern, intensity, and position of this ensemble of peaks rather than a single, large shift of one specific band.

ISSN 3030-3907

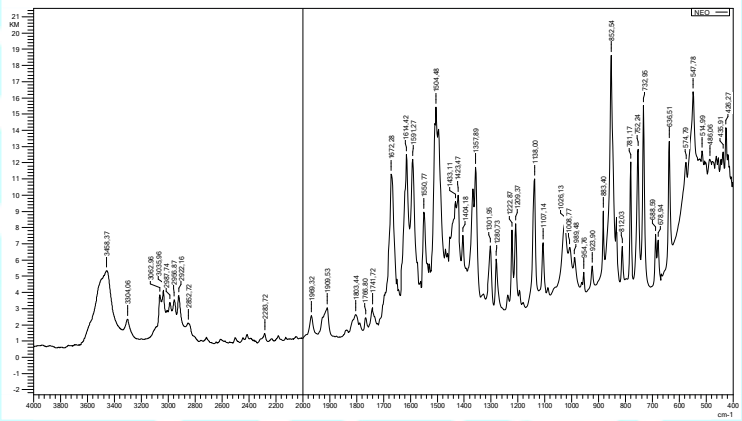


Figure 2. Infrared spectra of neocuproine

The IR spectrum of the aqua complex (Figure 3) was analyzed to confirm the coordination of neocuproine and water, and to verify the absence of urea.

The spectrum of $Co[(neo)_2(aqua)_2](formate)_2$ retains the characteristic "fingerprint" of the neocuproine ligand. The key ring-stretching vibrations are present, notably at 1593.03 cm^{-1} and 1504.42 cm^{-1}, showing minimal shift from their positions in the free ligand (1591.57 and 1504.38 cm^{-1}, respectively). More significantly, these peaks exhibit a marked increase in intensity relative to the free ligand spectrum. The persistence of this pattern, coupled with the intensity enhancement, is a strong indicator that neocuproine is acting as a chelating ligand, bound to the cobalt center through its two nitrogen atoms [10].

Definitive evidence for coordinated water (aqua ligands) is present in two regions of the spectrum. A broad absorption band centered at 3447.16 cm^{-1} is assigned to the O-H stretching vibrations of coordinated water, which is typically broadened and shifted to lower frequencies compared to free water due to hydrogen bonding in the solid state. More conclusively, a distinct peak is observed at 1667.74 cm^{-1}. This band falls squarely within the characteristic region for the H-O-H bending (scissoring) mode of coordinated water (~1600-1650 cm^{-1}) [11]. The presence of this bending mode is a definitive spectroscopic signature of coordinated water molecules in the complex.

The spectrum of Complex 1 shows no peak near 1660 cm^{-1} that can be assigned to the free urea C=O stretch. The peak at 1667.74 cm^{-1} is unequivocally assigned to the water bending mode. This confirms that urea is not a ligand in this complex, which is consistent with its formulation as an aqua complex.

The presence of the formate counterion is inferred from the peaks in the carbonyl stretching region. The asymmetric COO^- stretch typically appears between 1550 and 1650 cm^{-1}, and the peaks observed here are consistent with an ionic, non-coordinating formate group.

ISSN 3030-3907

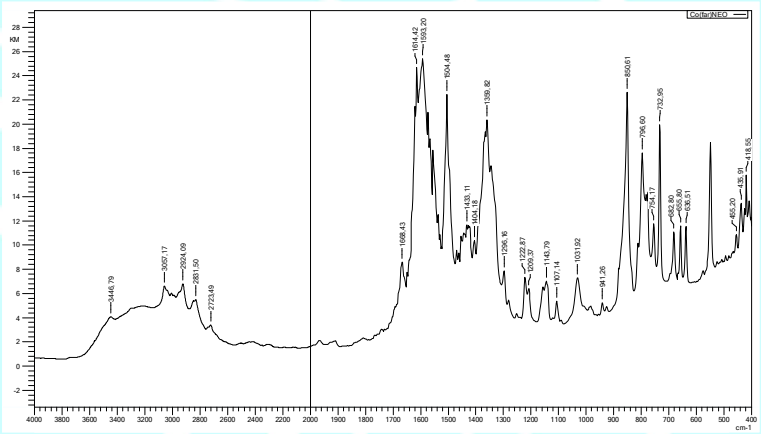


Figure 3. Infrared spectra of Co[(neo)$_2$(aqua)$_2$](formate)$_2$

The IR spectrum of the urea complex was scrutinized to confirm the coordination of both neocuproine and urea, and to determine the mode of urea coordination.

As in Co[(neo)$_2$(aqua)$_2$](formate)$_2$, the spectral signature of coordinated neocuproine is clearly evident. Peaks corresponding to the C=N/C=C ring stretches are present at 1592.44 cm^{-1} and 1504.26 cm^{-1}, confirming that neocuproine maintains its role as a bidentate N,N-donor ligand in this complex as well.

The spectrum reveals a dramatic change in the carbonyl stretching region compared to free urea. The sharp, single peak at 1660.26 cm^{-1} in free urea is replaced by a split and shifted profile, with strong, sharp peaks at 1632.34 cm^{-1} and 1681.32 cm^{-1}. The peak at 1632.34 cm^{-1} represents a significant downward shift of approximately 28 cm^{-1}. This negative shift is the classic indicator of carbonyl oxygen coordination [11]. The coordination of the oxygen lone pair to the Lewis acidic cobalt center reduces the electron density in the C=O bond, weakening its force constant and consequently lowering its vibrational frequency. The presence of multiple peaks can be attributed to the symmetric and asymmetric coupling of C=O stretches from the two distinct urea ligands in the complex or factor group splitting in the solid state. Supporting evidence is found in the N-H stretching region, where the sharp peaks of free urea are replaced by a new set of broader, shifted peaks at 3198.43 cm^{-1}, 3342.11 cm^{-1}, and 3404.15 cm^{-1}. This shift and broadening are consistent with coordination-induced changes in the hydrogen-bonding network and the electron density on the nitrogen atoms.

There is no distinct, isolated peak in the ~1650 cm^{-1} region that can be assigned to the bending mode of coordinated water. The features in this region are fully accounted for by the coordinated urea and the formate ion. The broad absorptions in the 3198-3404 cm^{-1} range are assigned to the N-H stretches of urea, not O-H stretches. This confirms the absence of coordinated water in Complex 2.

ISSN 3030-3907

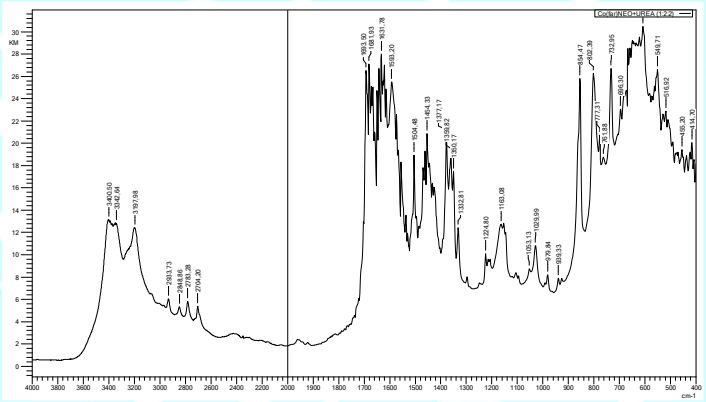


Figure 4. Infrared spectra of $Co[(neo)_2(urea)_2](formate)_2$

A summary of the key IR data and their assignments is provided in Table 1.

Table 1.

Key IR spectral data (cm^{-1}) and assignments for the free ligands and cobalt complexes.

Compound	ν(C=O) Urea / δ(H-O-H) Water	ν(C=N/C=C) Neocuproine	ν(N-H) Urea / ν(O-H) Water	Assignment
Urea	1660.26	-	3265-3503	Free ligand references
Neocuproine	-	1504, 1592, 1614	-	Free ligand references
$Co[(neo)_2(aqua)_2](formate)_2$	1667.74	1504, 1593	3447 (br)	δ(H-O-H) coordinated H_2O; Coordinated neo; ν(O-H) coordinated H_2O
$Co[(neo)_2(urea)_2](formate)_2$	1632.34, 1681.32	1504, 1592	3198-3404	ν(C=O) coordinated urea (O-mode); Coordinated neo; ν(N-H) coordinated urea

Results and discussion of the elemental analysis. Results are summarized in Table 2. Theoretical values were calculated from the empirical formulas $CoC_{32}H_{34}N_8O_6$ (a) and $CoC_{30}H_{30}N_4O_6$ (b) and compared with the experimental mass percentages measured by WD-XRF.

For both complexes the experimentally determined mass percentages match the theoretical values extremely well. Deviations between theoretical and experimental values are small for every element (typically within 0.06–0.07 mass% for the major elements and ≤0.1 mass% for cobalt), which indicates that the isolated solids correspond closely to the proposed empirical formulas and that the

ISSN 3030-3907

stoichiometry of the prepared complexes is essentially quantitative within analytical uncertainty.

Specifically, cobalt—the diagnostic element for confirming metal stoichiometry—shows near-perfect agreement: 8.60% (theoretical) vs 8.54% (experimental) for complex (a), and 9.80% vs 9.75% for complex (b). These results support the assigned metal:ligand ratios and indicate that cobalt is present in the expected amount for both formulations.

Carbon and hydrogen likewise show excellent agreement. Carbon is 56.06% theoretical vs 56.01% experimental for (a), and 59.90% vs 59.85% for (b). Hydrogen values are 5.00% vs 4.94% (a) and 5.03% vs 4.97% (b). These small, systematic negative offsets in H (≈0.06 mass%) are modest and typical for microanalytical methods where slight loss of volatile species or minor absorption differences can occur during sample preparation or instrument measurement.

Nitrogen and oxygen values also closely follow theoretical expectations. For (a), N: 16.34% (theoretical) vs 16.28% (experimental); O: 14.00% vs 13.94%. For (b), N: 9.32% vs 9.26%; O: 15.95% vs 15.89%. The very small negative deviations for O and N (≤0.06 mass%) are within typical analytical uncertainty for WD-XRF on light elements and do not indicate significant compositional disorder.

The WD-XRF measurement reports low impurity levels of 0.29% (complex a) and 0.28% (complex b). These impurity levels are minor and consistent with high chemical purity of the isolated products. Potential origins of the small impurity fraction include residual solvent or adventitious surface contamination, trace inorganic salts originating from reagents, or small amounts of unremoved side products. Given the small magnitude of the impurities, they are unlikely to affect the bulk chemical or coordination properties of the samples.

Table 2.

Elemental analysis of complexes $Co[(neo)_2(urea)_2](formate)_2$ (a) and $Co[(neo)_2(aqua)_2](formate)_2$ (b)

Element	Empirical formula of the complex			
	$CoC_{32}H_{34}N_8O_6$ (a)		$CoC_{30}H_{30}N_4O_6$ (b)	
	Theoretical mass percentage (%)	Experimental mass percentage (%)	Theoretical mass percentage (%)	Experimental mass percentage (%)
Co	8.60	8.54	9.80	9.75
C	56.06	56.01	59.90	59.85
H	5.00	4.94	5.03	4.97
N	16.34	16.28	9.32	9.26
O	14.00	13.94	15.95	15.89

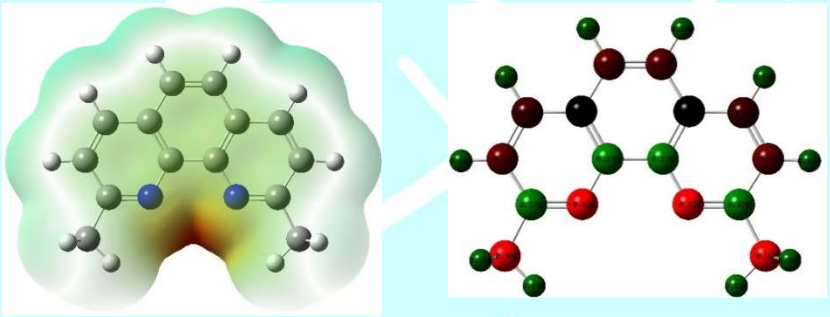
ISSN 3030-3907

Impurities	-	0.29	-	0.28

Quantum chemical studies of the ligands and complexes. This study utilized quantum chemical calculations to investigate the electronic properties of neocuproine (neo) and urea ligands, along with their cobalt(II) complexes, $Co[(neo)_2(aqua)_2](formate)_2$ and $Co[(neo)_2(urea)_2](formate)_2$.

To identify potential coordination sites, the electronic properties of the neocuproine and urea ligands were analyzed. Molecular Electrostatic Potential (ESP) maps, which visualize electron-rich (red) and electron-poor (blue) regions, were employed for this purpose.

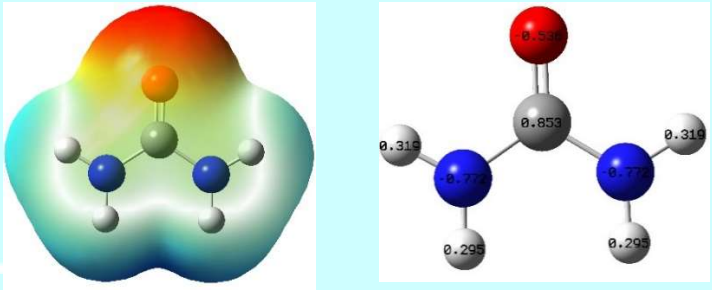
For neocuproine, the ESP map (Figure 5A) reveals the most negative potential (intense red) is localized on the two nitrogen atoms of the 1,10-phenanthroline ring. This high electron density, arising from the nitrogen lone pairs, identifies these sites as the primary nucleophilic centers, making them ideal for coordinating with the electron-deficient Co(II) metal center. This is corroborated by the Mulliken charge analysis (Figure 5B), which confirms that the nitrogen atoms bear the most significant negative charge.



A B

Figure 5. Graphical representation of electrostatic potential map(A) and Mulliken charges(A) of neocuproine

Similarly, the ESP map for urea (Figure 6A) indicates the highest electron density is concentrated on the carbonyl oxygen atom. The Mulliken charge of -0.536 on this oxygen (Figure 6B) supports this observation, identifying the carbonyl oxygen as the primary coordination site (Lewis base).

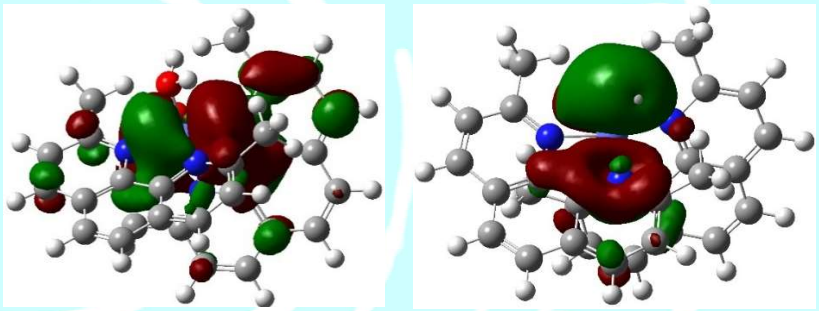


A B

Figure 6. Graphical representation of electrostatic potential map(A) and Mulliken charges (B) of urea

ISSN 3030-3907

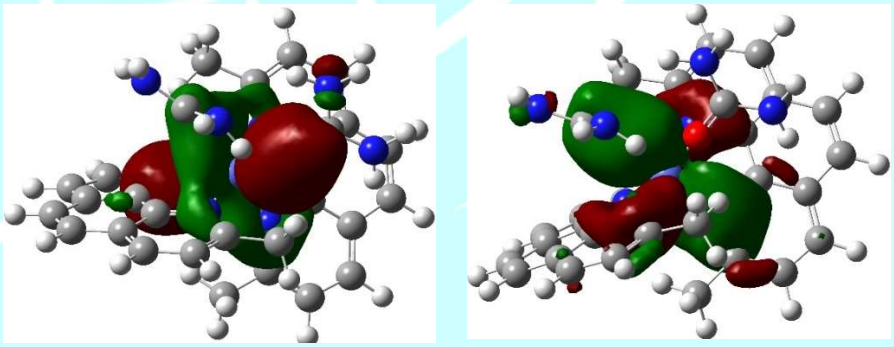
The Highest Occupied Molecular Orbital (HOMO) and Lowest Unoccupied Molecular Orbital (LUMO) are critical for understanding the chemical reactivity and electronic properties of molecules. For both the $Co[(neo)_2(aqua)_2](formate)_2$ (Figure 8) and $Co[(neo)_2(urea)_2](formate)_2$ (Figure 8) complexes, the HOMO and LUMO densities are primarily localized on the central cobalt atom and the neocuproine ligands.



A B

Figure 7. Graphical representation of HOMO (A) and LUMO (B) orbitals of $Co[(neo)_2(aqua)_2](formate)_2$ complex

This orbital distribution indicates that the primary electronic transitions, such as those involved in UV-Vis absorption, will be of the metal-to-ligand charge transfer (MLCT) type. The distribution of these frontier orbitals is crucial in determining the reactivity and kinetic stability of the complexes.



A B

Figure 8. Graphical representation of HOMO (A) and LUMO (B) orbitals of $Co[(neo)_2(urea)_2](formate)_2$ complex

Key quantum chemical parameters were calculated to quantitatively assess the properties of the ligands and complexes, as summarized in Table 3.

Table 3

Results obtained by quantum chemical calculation of ligands and complexes

Quantum chemical parameters	Neo	Urea	$Co[(neo)_2(aqua)_2](formate)_2$	$Co[(neo)_2(urea)_2](formate)_2$
E_{HOMO}, (Hartree)	-0.225	-0.230	-0.431	-0.389
E_{LUMO}, (Hartree)	-0.046	-0.085	-0.275	-0.264

ISSN 3030-3907

$\|\Delta E\| = E_{HOMO} - E_{LUMO}$, (Hartree)	0.179	0.145	0.156	0.125
Ionization energy, $I = -E_{HOMO}$, (Hartree)	0.225	0.230	0.431	0.389
Electron affinity, $A = - E_{LUMO}$, (Hartree)	0.046	0.085	0.275	0.264
Electronegativity, $\chi = (I + A)/2$ (Hartree)	0.135	0.158	0.353	0.326
Dipole momentum, μ (Debay)	2.32	4.23	5.65	4.19
Electron energy, (Hartree)	-646.66	-224.01	0.514	0.538

The HOMO-LUMO energy gap ($|\Delta E|$) is a significant indicator of chemical reactivity and molecular stability. A smaller energy gap implies higher chemical reactivity and lower kinetic stability, as less energy is required for electronic excitation. The calculated $|\Delta E|$ for the $Co[(neo)_2(urea)_2](formate)_2$ complex (0.125 Hartree) is notably smaller than that of the $Co[(neo)_2(aqua)_2](formate)_2$ complex (0.156 Hartree). This suggests that the substitution of aqua ligands with urea increases the overall reactivity of the complex. This increased reactivity may be attributed to the stronger σ-donating and π-accepting capabilities of urea compared to water, which perturbs the d-orbital splitting of the cobalt center and narrows the frontier orbital gap.

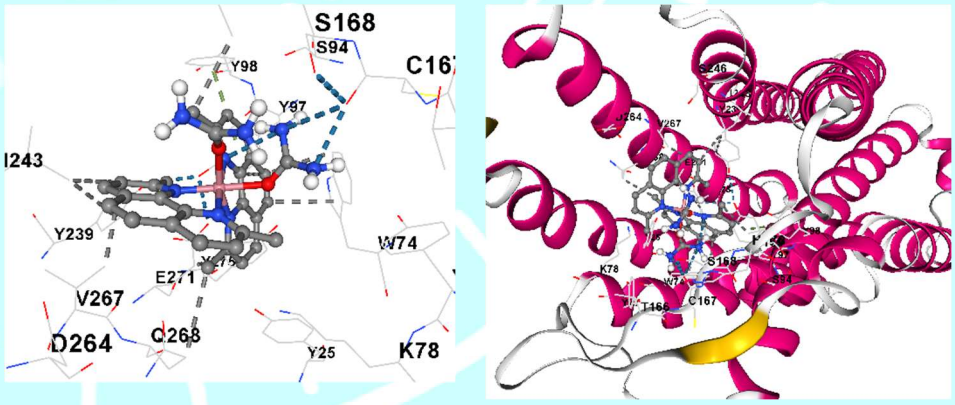
The ionization potential ($I = -E_{HOMO}$) and electron affinity ($A = -E_{LUMO}$) provide insight into the electron-donating and -accepting abilities. The $Co[(neo)_2(urea)_2](formate)_2$ complex possesses a lower ionization potential (0.389 Hartree) compared to its aqua analogue (0.431 Hartree), indicating it is a better electron donor. Correspondingly, the electronegativity (χ), which measures the ability to attract electrons, is slightly lower for the urea complex (0.326 Hartree) than for the aqua complex (0.353 Hartree), aligning with its greater tendency to release electron density.

The dipole moment (μ) measures the overall polarity of a molecule. The aqua complex exhibits a higher dipole moment (5.65 Debye) than the urea complex (4.19 Debye). This suggests that the coordination of urea ligands results in a more symmetric charge distribution within the complex compared to the coordination of water molecules.

ISSN 3030-3907

Finally, the calculated electronic energy provides a measure of relative thermodynamic stability. The $Co[(neo)_2(urea)_2](formate)_2$ complex has a slightly higher electronic energy (0.538 Hartree) than the $Co[(neo)_2(aqua)_2](formate)_2$ complex (0.514 Hartree). This suggests that the aqua complex is marginally more stable from a thermodynamic standpoint under the calculation conditions. However, the significantly increased reactivity (lower $|\Delta E|$) of the urea complex is often a more critical factor in determining its utility in chemical processes.

Docking Studies. To investigate the potential inhibitory activity of the synthesized cobalt(II) mixed-ligand neocuproine complexes, molecular docking studies were performed against the C-C chemokine receptor type 1 (CCR1). The study employed a two-step computational approach: an initial blind docking to identify potential binding sites, followed by a traditional, focused docking to refine the binding poses and calculate binding affinities.



A B

Figure 9. Blind docking's most favorable pose for $Co[(neo)_2(urea)_2](formate)_2$

A blind docking was first performed using Cb-dock to scan the entire receptor surface and identify the most probable binding sites. The results for both complexes are summarized in Table 4 and Table 5.

Table 4

Blind docking results for $Co[(neo)_2(urea)_2](formate)_2$

Cavities volume (Å3)	Center coordinates (x, y, z)	Size coordinates (x, y, z)	Vina score (kcal/mol)
1450	115, 143, 133	21, 21, 21	-8.3
294	107,129, 102	21, 21, 21	-7.2
1000	109, 119, 107	21, 21, 21	-7.1
491	105, 148, 134	21, 21, 21	-6.1
94	124, 124, 108	21, 21, 21	-5.3

ISSN 3030-3907

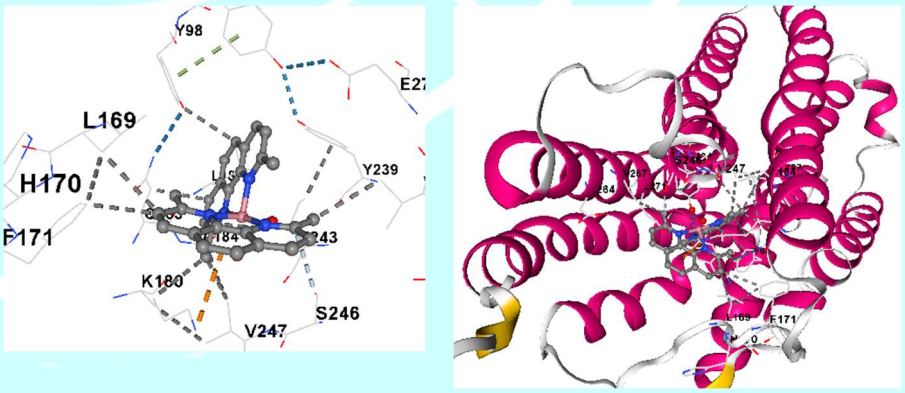
This analysis identified five distinct cavities on the CCR1 receptor. For both complexes, the largest cavity (volume 1450 Å³) yielded the most favorable (most negative) Vina score, indicating it is the likely primary binding pocket.

Table 5

Blind docking results for Co[(neo)$_2$(aqua)$_2$](formate)$_2$

Cavities volume (Å3)	Center corrdinates (x, y, z)	Size coordinates (x, y, z)	Vina score (kcal/mol)
1450	115, 143, 133	20, 20, 20	-9.8
1000	109, 119, 107	20, 20, 20	-8.9
294	107,129, 102	20, 20, 20	-8.7
491	105, 148, 134	20, 20, 20	-7.5
94	124, 124, 108	20, 20, 20	-6.9

For Co[(neo)$_2$(urea)$_2$](formate)$_2$, the best Vina score in this primary cavity was -8.3 kcal/mol (Table 4). For Co[(neo)$_2$(aqua)$_2$](formate)$_2$, the binding score in the same cavity was -9.8 kcal/mol (Table 5). These preliminary blind docking results suggest that while both complexes favor the same binding site.



A B

Figure 10. Blind docking's most favorable pose for Co[(neo)$_2$ (aqua)$_2$] (formate)$_2$

Following the identification of the primary binding site, a more precise, traditional docking was performed using AutoDock Vina to analyze the binding affinities and predict the inhibition constants (Ki). The results for the top 10 binding poses for each complex are detailed in Table 6.

ISSN 3030-3907

Table 6

Docking results for $Co[(neo)_2(urea)_2](formate)_2$ and $Co[(neo)_2(aqua)_2](formate)_2$

Poses	*$Co[(neo)_2(urea)_2](formate)_2$*			*$Co[(neo)_2(aqua)_2](formate)_2$*		
	Affinity (kcal/mol)	Ki (μM)	Ligand efficiency	Affinity (kcal/mol)	Ki (μM)	Ligand efficiency
1	-8.2	0.976	-0.20	-9.8	0.0656	-0.28
2	-8.1	1.16	-0.20	-9.6	0.0919	-0.27
3	-7.7	2.27	-0.19	-9.5	0.1088	-0.27
4	-7.5	3.18	-0.18	-9.0	0.2529	-0.26
5	-7.3	4.46	-0.18	-8.7	0.4196	-0.25
6	-7.2	5.28	-0.18	-8.3	0.8243	-0.24
7	-7.2	5.28	-0.18	-7.9	1.62	-0.23
8	-7.2	5.28	-0.18	-7.8	1.92	-0.22
9	-7.2	5.28	-0.18	-7.8	1.92	-0.22
10	-7.2	5.28	-0.18	-7.7	2.27	-0.22

The focused docking results strongly reinforce the findings from the blind dock. $Co[(neo)_2(urea)_2](formate)_2$ (Table 6): The best-ranked pose (Pose 1) exhibited a binding affinity of -8.2 kcal/mol. This corresponds to a predicted inhibition constant (Ki) of 0.976 μM and a ligand efficiency of -0.20.

$Co[(neo)_2(aqua)_2](formate)_2$ (Table 6): The best-ranked pose (Pose 1) showed a binding affinity of -9.8 kcal/mol. This affinity translates to a Ki of 0.0656 μM (or 65.6 nM) and a ligand efficiency of -0.28.

The computational results from both docking methods indicate that both synthesized complexes are effective binders to the CCR1 receptor.

The $Co[(neo)_2(urea)_2](formate)_2$ complex demonstrates significant binding capability (Table 6). Its best-ranked pose shows a binding affinity of -8.2 kcal/mol. This translates to a predicted inhibition constant (Ki) of 0.976 μM, positioning it as a potent near-micromolar inhibitor of CCR1. This level of activity is a strong indicator of therapeutic potential.

The $Co[(neo)_2(aqua)_2](formate)_2$ complex (Table 7) also demonstrates a high degree of binding. It returned a binding affinity of -9.8 kcal/mol. This strong affinity corresponds to a predicted Ki of 0.0656 μM (or 65.6 nM), identifying it as a highly potent sub-micromolar inhibitor.

CONCLUSION

Two mixed-ligand cobalt(II)-formate complexes incorporating neocuproine have been successfully synthesized and thoroughly characterized. The spectroscopic and elemental analyses substantiated the proposed structures, unveiling a coordination sphere in which neocuproine functions as a bidentate N,N-

ISSN 3030-3907

donor, added by either aqua or urea ligands. Quantum chemical investigations have elucidated their electronic characteristics, revealing that the replacement of water with urea ligands leads to a complex exhibiting enhanced chemical reactivity, as evidenced by a reduced HOMO-LUMO gap. Moreover, molecular docking simulations confirmed that both complexes serve as high-affinity binders to the CCR1 receptor, with the aqua complex demonstrating especially strong sub-micromolar inhibitory potential. The results underscore the considerable impact of the auxiliary ligand on the electronic configuration and biological efficacy of the complexes, establishing them as noteworthy subjects for further exploration in the realms of medicinal chemistry and materials science.

ACKNOWLEDGEMENTS

The manuscript was translated from Uzbek to English and grammatically polished with the help of artificial intelligence models under the supervision of the authors [12]. The scientific content, experimental work, data analysis, interpretation, and conclusions are entirely the original work of the authors.

REFERENCES:

1. H. Hu, "catena-poly[[aqua(1,10-phenanthroline)cadmium(ii)]-μ-benzene-1,4-dicarboxylato]", Acta Crystallographica Section E Structure Reports Online, vol. 65, no. 1, p. m90-m90, 2008. https://doi.org/10.1107/s1600536808041913

2. J. Yang, J. Ma, Y. Liu, J. Ma, & S. Batten, "Organic-acid effect on the structures of a series of lead(ii) complexes", Inorganic Chemistry, vol. 46, no. 16, p. 6542-6555, 2007. https://doi.org/10.1021/ic700613c

3. Q. Ma, M. Zhu, C. Yuan, S. Feng, L. Lu, & Q. Wang, "A molecular helix: self-assembly of coordination polymers from d10 metal ions and 1,10-phenanthroline-5,6-dione (pdon) with the bridges of scn− and cl− anions", Crystal Growth & Design, vol. 10, no. 4, p. 1706-1714, 2010. https://doi.org/10.1021/cg901297y

4. G. Accorsi, A. Listorti, K. Yoosaf, & N. Armaroli, "1,10-phenanthrolines: versatile building blocks for luminescent molecules, materials and metal complexes", Chemical Society Reviews, vol. 38, no. 6, p. 1690, 2009. https://doi.org/10.1039/b806408n

5. B. Harbuzaru, A. Corma, F. Rey, J. Jordá, D. Ananias, L. Carloset al., "A miniaturized linear ph sensor based on a highly photoluminescent self-assembled europium(iii) metal–organic framework", Angewandte Chemie, vol. 48, no. 35, p. 6476-6479, 2009. https://doi.org/10.1002/anie.200902045

6. L. Fan, C. Li, Z. Meng, & M. Tong, "Metal-mediated one-step in situ oxidation of 2,9-dimethyl-1,10-phenanthroline and formation of transition-metal and lanthanoid complexes", European Journal of Inorganic Chemistry, vol. 2008, no. 25, p. 3905-3909, 2008. https://doi.org/10.1002/ejic.200800499

7. Nakamoto, K. (2009). Infrared and Raman Spectra of Inorganic and Coordination Compounds, Part B (6th ed.). Wiley., p 74.
8. Bellamy, L. J. (1975). The Infrared Spectra of Complex Molecules (3rd ed.). Chapman and Hall., p 258.
9. Lever, A. B. P. (1968). Inorganic Electronic Spectroscopy. Elsevier., p 339.
10. Geary, W. J. (1971). The use of conductivity measurements in organic solvents for the characterisation of coordination compounds. Coordination Chemistry Reviews, *7*, p 81-122.
11. Ferraro, J. R. (1971). Low-Frequency Vibrations of Inorganic and Coordination Compounds. Plenum Press., p 152.
12. Quillbot. (2025). Quillbot (Version 1.3.2.0). https://quillbot.com/

ISSN 3030-3907